Environmental Research Letters

LETTER

Camouflaged as degraded wax: hygroscopic aerosols contribute to leaf desiccation, tree mortality, and forest decline

Juergen Burkhardt[1,7], Daniel Zinsmeister[1], David A Grantz[1,2], Sonia Vidic[3], Mark A Sutton[4], Mauricio Hunsche[5,6] and Pariyar Shyam[1,6]

1 University of Bonn, Institute of Crop Science and Resource Conservation, Plant Nutrition Group, Karlrobert-Kreiten-Str. 13, D-53115 Bonn, Germany
2 Department of Botany and Plant Sciences, University of California at Riverside, Kearney Agricultural Center, Parlier, CA 93648, United States of America
3 Meteorological and Hydrological Service, Air Quality Division, HR-10000 Zagreb, Croatia
4 Centre of Ecology and Hydrology, Edinburgh Research Station, Midlothian EH26 0QB, United Kingdom
5 COMPO EXPERT GmbH, Krögerweg 10, D-48155, Münster, Germany
6 University of Bonn, Institute of Crop Science and Resource Conservation, Horticultural Science Group, Auf dem Hügel 6, D-53121 Bonn, Germany
7 Author to whom any correspondence should be addressed.

E-mail: j.burkhardt@uni-bonn.de

Keywords: aerosol pollution, Anthropocene, desiccant, forest decline, silver fir, tree mortality, VPD

Supplementary material for this article is available online

OPEN ACCESS

RECEIVED
12 April 2018

REVISED
11 July 2018

ACCEPTED FOR PUBLICATION
13 July 2018

PUBLISHED
25 July 2018

Abstract

Some 40 years ago, air pollution caused widespread forest decline in Central Europe and eastern North America. More recently, high levels of tree mortality worldwide are thought to be driven by rising temperatures and increasing atmospheric drought. A neglected factor, possibly contributing to both phenomena, is the foliar accumulation of hygroscopic aerosols. Recent experiments with experimentally added aerosols revealed that foliar aerosol accumulation can (i) create the microscopic impression of 'wax degradation', considered an important proxy of forest decline associated with air pollution, though the mechanism remains unexplained; and (ii) increase epidermal minimum conductance (g_{min}), a measure of cuticular permeability and completeness of stomatal closure—both could lead to reduced drought tolerance. Here, those studies with applied aerosol are extended by addressing plant responses to reduction of ambient aerosol.

Scots pine, silver fir, and common oak seedlings were grown for 2 years in greenhouses ventilated with ambient air (AA) or air filtered to remove nearly all aerosol particles (FA). Removal of ambient aerosol prevented the development of amorphous structures viewed in the electron microscope that have typically been interpreted as degraded waxes. Lower g_{min} values suggested that FA plants had better stomatal control and therefore greater drought tolerance than AA plants. The co-occurrence of apparent wax degradation and reduced drought tolerance in AA plants suggests a common cause. This may be mediated by the deliquescence and spreading of hygroscopic aerosols across the leaf surface. The liquid film produced may penetrate the stomata and facilitate unproductive stomatal transpiration. In this way, aerosol pollution may enhance the impacts of atmospheric drought, and may damage trees and forests on large spatial scales.

Introduction

Two large-scale forest diebacks have been attributed to atmospheric factors. Both have affected remote regions, in both cases biotic factors have been ruled out as primary drivers, and yet these dieback events appear to be independent. Starting from the 1970s, forest decline by air pollution (FDAP) affected trees in Europe and eastern North America, which was linked to industrial

and combustion emissions of SO_2, NO_x, and resulting acids (Johnson and Siccama 1983, McLaughlin 1985, Schütt and Cowling 1985). However, while the phenomenon was intensively studied for about 20 years, no coherent mechanism for the decline was identified (Bussotti and Ferretti 1998, Schulze 1989, Ulrich 1990). Although regulatory action improved air quality, forest health was not completely restored. Recurrent die-off events have tended to follow drought events (Klap *et al* 2000, Vacek *et al* 2015). Although drought has not been considered a major contributor to FDAP, seemingly anomalous drought-related symptoms are observed as a component of responses to pollutants. A well-documented example is the reduced drought tolerance of silver fir (*Abies alba* Mill.), associated with relatively low levels of SO_2 from distant sources. Drought-like symptoms such as needle loss, reduced expansion of growth rings, and early dieback were correlated with the sulfur content of the needles—and improved when SO_2 emissions decreased (Elling *et al* 2009). Thus, there may be unrecognized interaction between FDAP and drought.

Tree mortality by hotter drought (TMHD), the second attributed cause of large-scale dieback, has been discussed since the beginning of this century, in arid and semi-arid regions of western North America and worldwide (Allen *et al* 2015, Bigler *et al* 2006, Breshears *et al* 2005, Buras *et al* 2018, van Mantgem *et al* 2009, Patrut *et al* 2018). It is a manifestation of global warming, that exposes plants to linear increases in temperature but exponential increases in atmospheric drought (evaporative demand; vapor pressure deficit, VPD) (Novick *et al* 2016, Williams *et al* 2013). This accelerates transpiration and challenges plant hydraulic systems. Hydraulic failure is associated with drought-induced mortality across multiple tree taxa (Adams *et al* 2017).

Air pollution has not generally been considered a contributing factor to TMHD. 'Carbon starvation' was suggested to increase mortality during drought by restriction of CO_2 uptake by stomatal closure (McDowell *et al* 2008). This appeared to explain the anomalous observation that species reacting most sensitively to drought by stomatal closure (i.e. drought resistant) were most affected by TMHD (i.e. drought sensitive), as in the classic example of the juniper-pinon pine system (McDowell *et al* 2008). However, the 'carbon starvation' hypothesis is not consistent with observed patterns of non-structural carbohydrate reserves associated with mortality (Adams *et al* 2017).

Here we suggest a novel reconciliation of these diverse observations. Both types of forest decline may be linked mechanistically by the accumulation and hygroscopic action of aerosols deposited on leaves. The global increase of atmospheric aerosol concentrations is an indicator of the Anthropocene (Andreae 2007, Steffen *et al* 2015). Aerosols are ubiquitous and increasingly hygroscopic, and are readily deposited on trees (Burkhardt and Grantz 2017). *In situ* measurements of electrical leaf surface conductance (Burkhardt and Eiden 1994) and direct observation (Burkhardt *et al* 2001, Grantz *et al* 2018) indicated the existence of thin water films on needles and leaves caused by deliquescence (absorption of water by hygroscopic aerosol). These solutions overcome cuticular hydrophobicity and creep into individual stomata (Burkhardt *et al* 2012, Burkhardt and Hunsche 2013, Eichert *et al* 2008, Huang and Huang 1976, van Enckevort and Los 2013). By this 'hydraulic activation of stomata' (HAS; Burkhardt 2010), a thin liquid film (< 100 nm) can form a connection between the leaf surface and the leaf apoplast that normally forms the end of the plant hydraulic system (figure 1). We hypothesize that by the establishment of this liquid connection, the plant hydraulic system is extended to the leaf surface, enabling bidirectional liquid water transport through the stomatal pores, according to water potential gradients. In daytime, HAS may generate additional transpiration with water evaporating from the outer leaf surface as well as through the stomatal pores (figure 1). Partial stomatal closure has no effect on evaporation from the leaf surface, and little impact on transport of liquid water through the pores. This may reduce stomatal control of water loss (Burkhardt 2010) and contribute to hydraulic failure in TMHD. Furthermore, this deposition may lead to the appearance of 'degraded wax' that has been considered diagnostic of FDAP (Burkhardt and Pariyar 2014, Trimbacher and Weiss 1999, Turunen and Huttunen 1990).

These effects of aerosol deposition have been demonstrated experimentally by application of aerosol to diverse plant species (Burkhardt *et al* 2001, Burkhardt and Pariyar 2014, 2016). Similarly, exclusion of ambient aerosol reduced the epidermal minimum conductance (g_{min}) of short-lived faba bean leaves, and reduced water flux per directly measured stomatal aperture (Burkhardt and Pariyar 2014, 2016, Grantz *et al* 2018). Here we test these concepts using the exclusion of ambient aerosol from long-lived tree needles.

Methods

Plants and greenhouses

Potted individuals of Scots pine (*Pinus sylvestris* L.), Silver fir (*Abies alba* Mill.), and Common Oak (*Quercus robur* L.) seedlings were used for the study which ran from 2015 to 2017. In 2015, pine seedlings were 6 years and 110 cm tall, fir 4 years and 30 cm tall, and oak 3 years and 70 cm tall. Oak and fir were planted in 15 cm (dia.) × 20 cm (ht.) pots. Pine was planted in 25 cm × 33 cm pots. All pots contained potting mix (Profi Substrat; Einheitserde, Typ Topf). From March to October, plants were fertilized every other week with complete nutrient solution including micronutrients. Plants were irrigated as needed. Plants were randomly assigned to one of two adjacent research greenhouses at the University of Bonn, Germany (figure S1 available at stacks.iop.org/ERL/13/085001/mmedia

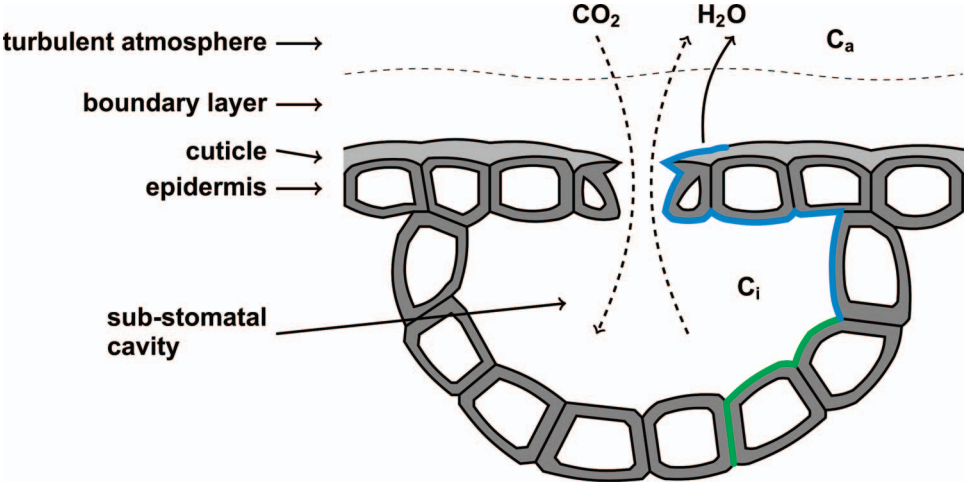

Figure 1. Hydraulic activation of stomata (HAS): liquid water forms by condensation to hygroscopic particles on the leaf surface, from where it creeps into the substomatal cavity (blue line; thickness probably < 100 nm) and connects with apoplastic liquid water (green line). In this way, the plant's hydraulic system is extended to the leaf surface. Liquid water reaches the leaf surface from where it evaporates (solid arrow), mostly independent of stomatal aperture. Dashed arrows, gas exchange. C_a and C_i: external and internal CO_2 concentrations.

for photo). Measurements were obtained discontinuously throughout 2 years, only using leaves and needles that had developed within the greenhouses.

One greenhouse was ventilated with ambient air (AA) and the other with filtered air (FA) from which nearly all particles were excluded, both with 2 air exchanges min^{-1}, as described previously (Pariyar *et al* 2013, Burkhardt and Pariyar 2016, Grantz *et al* 2018). Filtration of FA to HEPA (high efficiency particulate air) standards was achieved with a cloth bag followed by high efficiency filter pad (No. 13; ACS; Essen, Germany). Within the greenhouses, total aerosol number concentrations (> 10 nm) were measured by a cloud chamber condensation nuclei counter (TSI 3783; TSI, Shoreview, MN, USA). Total aerosol number concentration in AA was 6–7 $\times 10^9$ particles m^{-3}. In FA, by opening the door which briefly admitted ambient air, and by movement of personnel within the FA greenhouse, a few particles were admitted or resuspended from the floor and bench. Nevertheless particle number concentration was reduced to 5–10 $\times 10^6$ m^{-3}, i.e. reduced by > 98% as previously reported (Grantz *et al* 2018).

Elemental aerosol and trace gas concentrations in the greenhouses were collected throughout the entire year 2015 with monthly resolution by CEH DELTA low-volume denuder sampling systems (Tang *et al* 2009). Tubing and filters were removed monthly and sent to the Croatian Meteorological Service, Zagreb, Croatia for chemical analysis. The mean mass concentration of all ionic aerosol components was 4.90 $\mu g\, m^{-3}$ in the AA greenhouse (table 1, figure S2), about 28% of annual, ambient PM10 in 2016 (17.4 $\mu g\, m^{-3}$, monitored in a nearby monitoring station throughout 2016; LANUV, DENW062, Grantz *et al* 2018), in agreement with a recent study on European aerosol composition (Putaud *et al* 2010). After filtration, 0.67 $\mu g\ m^{-3}$ of ionic aerosol mass remained in the FA greenhouse (table 1, figure S2), a reduction to 13.7%. Filtration of aerosol mass was less effective than of particle number (Grantz *et al* 2018), probably reflecting the cut-off of aerodynamic diameter of the Delta filter (4–5 μm), thus excluding coarse particles with heavy mass, and the unknown rates of volatilization of NH_4NO_3 and NH_4Cl aerosols, and resuspension of coarse particles as mentioned above. The three most abundant ions were NO_3^-, contributing 45% (AA) and 43% (FA) to ionic aerosol mass, respectively; NH_4^+ (21% and 29%); and SO_4^{2-} (24% and 10%) (table 1). The aerosol concentration in the AA greenhouse was about half of that in the the atmosphere that caused FDAP in a remote forest site in 1988 (Ludwig and Klemm 1990, table 1); the earlier aerosol mix also had a different ion composition of 40% SO_4^{2-}, 30% NO_3^-, and 19% NH_4^+ (Ludwig and Klemm 1990). Relative to the damaging 1988 values, concentrations in the FA greenhouse were only 7% for overall ionic aerosol concentrations; 10% for NO_3^- and NH_4^+, respectively; and less than 2% for SO_4^{2-} (table 1).

For gas phase NH_3 and SO_2, mean AA and FA concentrations differed by less than 10% (table 2(*a*)); monthly AA and FA concentrations were highly correlated ($r^2 > 0.9$) and close to the 1:1 line (figures 2 and S3). For gas phase HNO_3 and HCl, mean AA and FA concentrations differed by less than 20% (table 2(*a*)). AA and FA concentrations of HNO_3 were highly correlated ($r^2 = 0.84$). Over the year, and particularly in summer, FA HNO_3 concentrations exceeded AA values by 19% ($p = 0.02$), resulting in a steep slope of the correlation (figures 2 and S3). Mean FA HCl concentrations also exceeded AA values by 19% but were less well correlated and not significantly enhanced ($r^2 = 0.31$; figure 2). Ozone (O_3) concentrations in the greenhouses were determined from April to October

Table 1. Mean ionic aerosol mass concentrations, measured in the AA and FA greenhouses throughout 2015 (see table S1 for concentrations in ppb). FDAP: reported ionic aerosol mass concentrations within a remote area affected by forest decline from air pollution, measured 1988 in northeastern Bavaria, Germany (Ludwig and Klemm 1990, rural site WF, all size classes combined). Ratios for Σ FDAP are calculated without K^+. Except calcium and magnesium, ions were statistically different between AA and FA, p(Na) = 0.03, others $p < 0.001$. Magnesium was just at the limit of detection.

Aerosols	FA ($\mu g\,m^{-3}$)	AA Fraction	FDAP ($\mu g\,m^{-3}$)	FA/ AA Fraction	AA/ FDAP ($\mu g\,m^{-3}$)	FA/ FDAP Fraction	(%)	(%)	(%)
NH_4^+	0.19	0.29	1.05	0.21	1.92	0.19	18.6	54.8	10.2
NO_3^-	0.29	0.43	2.22	0.45	2.95	0.30	12.9	75.3	9.7
SO_4^{2-}	0.07	0.10	1.20	0.24	3.92	0.40	5.6	30.5	1.7
Cl^-	0.04	0.05	0.21	0.04	0.49	0.05	16.6	43.3	7.2
Ca^{2+}	0.01	0.01	0.03	0.01	0.14	0.01	31.1	21.2	6.6
Mg^{2+}	0.02	0.03	0.02	0.01	0.04	0.00	124.6	37.4	46.7
Na^+	0.05	0.08	0.17	0.03	0.25	0.03	32.5	66.6	21.6
K^+	n.a.	n.a.	n.a.	n.a.	0.17	0.02	n.a.	n.a.	n.a.
Σ aerosols	**0.67**	1.00	**4.90**	1.00	9.88 (**9.71**)	1.00	**13.6**	**50.3**	**6.9**

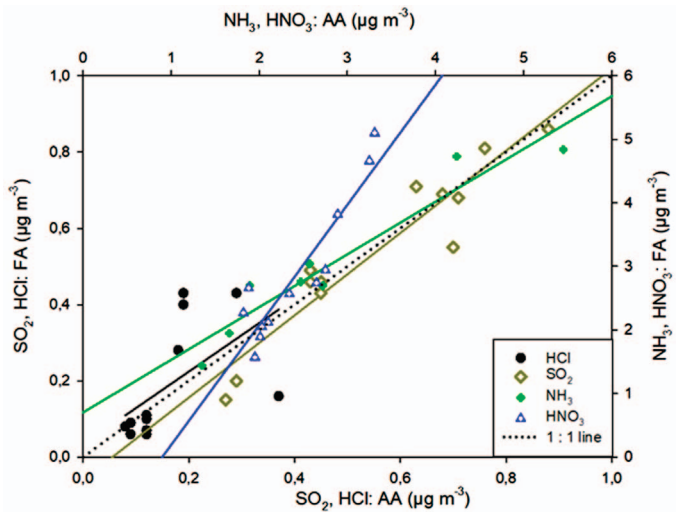

Figure 2. Trace gas concentrations in FA vs AA greenhouses, measured throughout 2015. Each data point represents a monthly average concentration. SO_2, HCl: left and bottom axes; NH_3, HNO_3: right and top axes.

2016. Hourly and annual trends were similar in the two greenhouses (Grantz *et al* 2018). Aerosol filtration caused a slightly warmer and drier environment in the FA compared to the AA greenhouse. Over the period of 2 years, the FA greenhouse was significantly warmer ($\Delta T = 0.67\,°C$), drier ($\Delta RH = 3.32\%$,), and with higher vapor pressure deficit ($\Delta VPD = 0.05$ kPa), respectively (table 2(*b*)).

Foliar rinsing

Fir twig segments with needles that had developed in the years 2016 (year 1) and 2015 (year 2) were cut from the seedlings. The segments were sealed at the cut ends with paraffin to prevent leaching. Each twig segment was transferred to a plastic beaker containing 60 ml of deionized water and shaken for 10 s by hand. Twigs were removed and the water samples were frozen (−28°C). Needles were separated and the projected leaf area determined photographically (ImageJ). The projected leaf area was doubled to obtain effective needle surface area. Ion concentrations were related to needle surface area.

Thawed wash water was filtered (0.45 μm) before chemical analysis. The NH_4^+ was analyzed with a continuous flow analyzer. The anions Cl^-, NO_3^-, SO_4^{2-}, and PO_4^{3-} were determined using High Performance Liquid Chromatography (HPLC; Dionex). The cations Ca, K, and Na were determined by Atomic Absorption Spectrometry. Manganese was analyzed by Inductively Coupled Plasma- Optical Emission Spectrometry (ICP-OES).

Minimum epidermal conductance (g_{min})

The g_{min} was determined from oak leaves in September 2015, from the youngest fir needles in November 2015, and from the youngest pine needles in November 2016. The cut ends were sealed with paraffin, and g_{min} determined from leaf drying curves as previously described (Burkhardt and Pariyar 2014, Grantz *et al* 2018).

Foliar carbon isotopes

Fir needle samples (1 and 2 years old) were obtained in April 2017 for determination of $\delta^{13}C$ values by mass spectrometry, following the procedure described earlier (Burkhardt and Pariyar 2016).

Table 2. Trace gas concentrations and environmental conditions and in the AA and FA greenhouses; (*a*) mean values of trace gases NH_3, HNO_3, SO_2, and HCl, measured throughout 2015 (April-June ammonia data missing - see table S2 for concentrations in ppb). (*b*) Mean values of T, RH, VPD, measured over a period of 2 years (May 2015-April 2017). *p* values calculated from (*a*) monthly values, (*b*) monthly means.

	FA	AA	FA/AA (%)	*p*
a) Trace gases				
NH_3 ($\mu g\,m^{-3}$)	3.02	2.79	108.2	n.s.
HNO_3 ($\mu g\,m^{-3}$)	2.87	2.42	118.6	0.02
SO_2 ($\mu g\,m^{-3}$)	0.54	0.56	96.4	n.s.
HCl ($\mu g\,m^{-3}$)	0.19	0.16	118.8	n.s.
Σ trace gases ($\mu g\,m^{-3}$)	**6.62**	**5.93**	**111.6**	**0.02**
b) Environment				
T (°C)	16.98	16.31	104.1	< 0.001
RH (%)	61.20	64.52	94.9	< 0.001
VPD (kPa)	0.75	0.70	107.1	< 0.001

Scanning electron microscopy

In October 2016, freshly excised twigs were obtained from fir, oak, and pine plants grown under AA and FA conditions, and brought into the laboratory. Oak leaves were sprayed in a wind tunnel for 4 hours as previously described (Burkhardt and Pariyar 2014), using an aerosol generator (ATM 220 Atomizer with DDU 570/H; Topas GmbH, Dresden, Germany) and 0.5 μm Na-fluorescein aerosol (75% RH deliquescence humidity, comparable to NaCl and ammonium sulfate; Burkhardt and Pariyar 2014, Burkhardt *et al* 1999). Single needles were separated and fixed to a specimen mount with double sided adhesive Leit tables. Needles were gold-coated by sputtering (Edwards Scancoat 6; 1.5 kV, 60 mA for 5 s). This provided a conductive layer on the plant material and enhanced observation of deposited material. The more delicate oak leaves were observed without sputtering. Leaves and needles were imaged using an environmental scanning electron microscope (ESEM; XL 30 FEI-Philips, Eindhoven, The Netherlands) in SEM mode, operated at 17 kV.

Statistics

Same age samples from AA and FA were compared to identify the effects of aerosol exclusion. Statistical analysis was performed using Sigma Plot (v. 13). For plant samples, data were checked for normality (Shapiro-Wilk test) and homogeneity of variance (Brown-Forsythe test). If both tests were passed, two-tailed Student's *t*-test was performed. When normality failed, a two-sided Mann-Whitney-U-test was used to evaluate between the two groups. Time series data (DELTA trace gas and aerosol samples; T, RH, VPD) were analyzed with a paired, two-tailed Student's *t*-test. The resulting *p*-values are presented.

Results

Aerosol deposition on fir needles

Ionic mass on the needle surface depended both on the aerosol environment as well as on needle age (table 3; figure S4). The overall amount of ionic mass was between 1.66 $\mu g\,cm^{-2}$ (1 year old FA needles, FA1) and 9.01 $\mu g\,cm^{-2}$ (2 year old AA needles, AA 2). The overall value of FA1 was 29.9% of the AA1 value, while FA2 was 56% of AA2. On all needle classes, nitrate was the ion contributing most to the aerosol mass, contributing about half in FA1, and about one third for all other needle classes (table 3). On a molar basis, potassium was the most abundant ion on 2 year old needles (figure S4). The strongest reduction from AA to FA for single ions were NH_4^+ (6.5% of AA) and Na^+ (6.6%) for 1 year old needles, while for 2 year old needles, PO_4^{3-} (32.0%) and SO_4^{2-} (32.9%) were most strongly reduced. Under FA compared with AA, the smallest reduction for 1 year old needles was found for nitrate (51.5% of AA) with the smallest reduction for 2 year old needles found for potassium (82.6% of AA; table 3; figure S4). Several cations and anions increased with leaf age, likely reflecting leaching as well as deposition (Tukey 1970). Manganese concentrations were higher on needles in the AA greenhouse and strongly increased with needle age (table 3, Figure S5).

Minimum epidermal conductance (g_{min})

The highest g_{min} was measured for AA oak leaves (0.475 $mmol\,m^{-2}\,s^{-1}$, table 4). The g_{min} of AA fir needles was 0.388 $mmol\,m^{-2}\,s^{-1}$ and of AA pine leaves, 0.130 $mmol\,m^{-2}\,s^{-1}$. The g_{min} decreased in all cases when aerosols were excluded. FA g_{min} was 78% of AA for oak, 81% for fir, and 77% for pine, respectively (table 4).

Foliar carbon isotopes

Carbon isotope discrimination differed significantly between AA and FA leaves of second year fir needles. AA samples had a less negative value than FA, indicating lower values of intercellular CO_2. Carbon isotopes for first year fir needles did not differ (table 5).

Scanning electron microscopy

There were few crystalline particles > 10 μm on the leaves and needles of silver fir. Some of these appeared to be the source, by deliquescence, of amorphous structures covering the tubular waxes (figure 3(*a*)). These were distinct from the native tubular wax structure in some areas, but were visually mixed in other areas as the salt solutions permeated the tubular wax structures (figure 3(*b*)). The identification of such deliquescent salts became possible only by following the decomposition

Table 3. Leaf surface ion concentrations per leaf area (mean ± SE), from silver fir needles of different age classes, determined by rinsing and subsequent chemical analysis. AA: ambient air; FA: filtered air; 1 and 2: needle age in years. Within rows, numbers followed by the same letter are not statistically different ($p > 0.05$). Sample size $n = 10$. ∗: manganese values are medians, given in ng cm^{-2}.

	FA1 (μg cm^{-2})	AA1 (μg cm^{-2})	FA2 (μg cm^{-2})	AA2 (μg cm^{-2})	FA1/AA1 (%)	FA2/AA2 (%)
Cl^-	0.18 ± 0.03 a	0.69 ± 0.15 c	0.34 ± 0.04 b	0.60 ± 0.04 c	25.8%	57.5%
SO_4^{2-}	0.11 ± 0.02 a	0.78 ± 0.09 c	0.44 ± 0.04 b	1.35 ± 0.07 d	14.5%	32.9%
NO_3^-	0.89 ± 0.18 a	1.73 ± 0.12 b	1.83 ± 0.21 b	2.90 ± 0.19 c	51.5%	63.1%
PO_4^{3-}	0.07 ± 0.01 a	0.55 ± 0.26 abc	0.29 ± 0.04 b	0.90 ± 0.11 c	11.9%	32.0%
NH_4^+	0.005 ± 0.002a	0.080 ± 0.009 b	0.115 ± 0.020 b	0.278 ± 0.026 c	6.5%	41.3%
K^+	0.30 ± 0.04 a	0.85 ± 0.21 b	1.70 ± 0.25 c	2.06 ± 0.22 c	35.5%	82.6%
Na^+	0.03 ± 0.01 a	0.48 ± 0.24 b	0.07 ± 0.02 a	0.19 ± 0.04 b	6.6%	38.4%
Ca^{2+}	0.08 ± 0.01 a	0.41 ± 0.02 c	0.24 ± 0.03 b	0.73 ± 0.04 d	18.8%	33.3%
Mn	0.00∗ a	3.38∗ b	6.16∗ c	14.90∗ d		
Σ	1.66 ± 0.24	5.57 ± 0.93	5.04 ± 0.42	9.01 ± 0.52	29.9%	56.0%

Table 4. Minimum epidermal conductance g_{min} (mmol m^{-2} s^{-1}) of one-year-old needles of fir and pine, and leaves of oak. Sample size (n) and statistical significance (p) values are shown.

	FA	AA	n	p
Fir	0.316 ± 0.015	0.388 ± 0.024	10	**0.023**
Pine	0.100 ± 0.011	0.130 ± 0.009	7	**0.017**
Oak	0.371 ± 0.017	0.475 ± 0.022	11	**0.003**

Table 5. Carbon isotope $\delta^{13}C$ values from fir needles of different ages (1-, 2 year old). Sample size $n = 10$. Values (mean ± SE), and statistical significance (p) values are shown.

	FA	AA	p
Fir year 1	−27.51 ± 0.22	−27.42 ± 0.19	0.745
Fir year 2	−27.46 ± 0.15	−26.98 ± 0.13	**0.023**

and spreading of the larger salt structures, illustrating the difficulties of distinguishing waxes from salts in SEM images.

In fir, the comparison between AA and FA needles showed clear differences. The FA needles lacked the amorphous structures that were found on AA. At low magnification, AA needles had more contrast and crystalline particles (figure 3(*c*)), whereas deposits on the FA needles appeared soft and were difficult to focus (figure 3(*d*)). However, at higher magnification, amorphous, crust-like structures were apparent in the stomatal regions of the AA needles, sometimes together with micron-sized crystalline particles (figure 3(*e*)) that were not observed on FA needles (figure 3(*f*)). Further magnification revealed details about the penetration and coverage of tubular waxes by the crust-like material (figures 3 (*g*)(AA), (*h*)(FA)). These spreading crusts appeared inside the stomatal antechamber of the AA needles, and gave the extremely fine tubular structures in this region a coarser appearance. Some of the fine voids in this area became blocked by crusts (figures 3 (*g*)−(*h*)).

Crust-like structures could also be recognized in the stomatal antechambers of AA needles of Scots pine (figure 4(*a*)) that were not found on FA needles (figure 4(*b*)). Less distinct differences were observed between FA leaves and AA leaves of oak (figures 4(*c*)−(*f*)). The surfaces of AA leaves (figure 4(*c*)) appeared more cluttered and with less contrast than FA leaves (figure 4(*d*)) in the SEM. At greater magnification (squares and arrowheads in figures 4(*c*) and (*d*)), crust-like structures were observed that produced a hazy appearance of the needle-like waxes in AA (figures 4(*e*): AA, (*f*): FA) and were responsible for low contrast in the AA SEM images (figures 4(*c*) and (*e*)). There were obvious differences between those oak leaves that had been sprayed with additional submicron aerosols (figure 4(*g*)) and untreated FA leaves (figure 4(*h*)). Waxes on the sprayed leaves appeared 'eroded' (figure 4(*g*)) compared to FA waxes (figure 4(*h*)). The rapidly developed symptoms demonstrated that the traditional interpretation of this morphology as wax degradation is not correct. The waxes had been covered by crusts of the deliquescent aerosols, giving the appearance of degraded wax.

Discussion

Scanning electron microscopy is the only technique by which 'wax degradation' has been identified and described. Air filtration prevented the formation of 'wax degradation' symptoms and was found to be associated with lower g_{min} of FA fir, pine, and oak seedlings. In a previous study with amendment by ammonium sulfate aerosol, the change from fine tubular waxes to an amorphous surface on pine needles was observed within a few minutes, induced by a short humidity cycle causing the salt to deliquesce, expand across the surface, and cover the tubular waxes (Burkhardt and Pariyar 2014). Here, the ambient, chemically diverse aerosol produced amorphous surfaces on AA leaves over the course of months, by a similar process: (i) the attraction of water vapor by hygroscopicity; (ii) the dissolution of the hygroscopic aerosol fraction; and (iii) their resulting mobility and distribution across the leaf surface, leading to coverage of tubular waxes by amorphous crusts with the typical appearance of 'wax degradation'.

Most aerosols are hygroscopic, attracting atmospheric humidity and enhancing condensation, similar to their function as cloud-condensation nuclei in the atmosphere (Petters and Kreidenweis 2007). On leaf surfaces, stomatal transpiration is an additional source of water vapor. Few deposited aerosols appear crystalline, separate, and large enough to be clearly recognized in SEM images; many others are too small

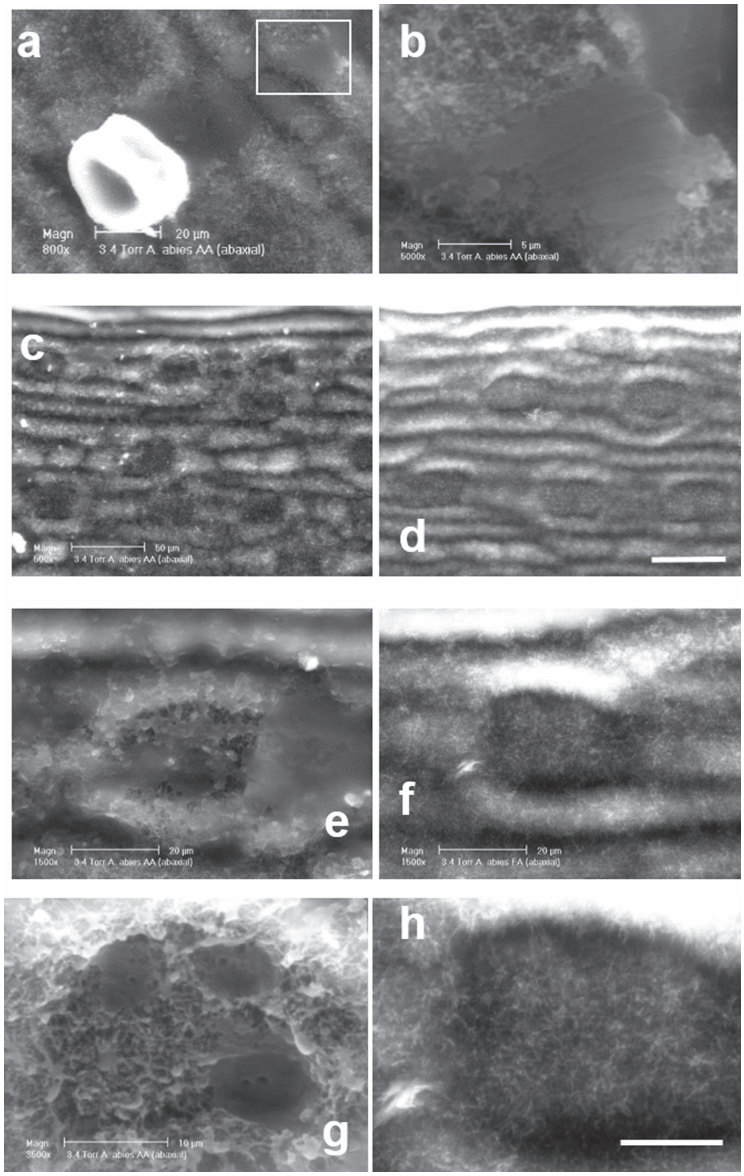

Figure 3. Scanning electron microscope (SEM) images of surfaces of silver fir needles. (*a*): Large aerosol particle dissolving on the surface of an AA needle. The white rectangle marks the area detailed in (*b*). (*c*), (*e*) and (*g*): Surface of a representative AA needle, showing amorphous structures derived from aerosol deposition. (*d*), (*f*) and (*h*): Surface of a representative FA needle. Scales: (*a*): 20 μm; (*b*): 5 μm; (*c*) and (*d*): 50 μm; (*e*) and (*f*): 20 μm; (*g*) and (*h*): 10 μm.

or poorly delimited to image clearly. Our experimental approach enabled the identification of deposited aerosols by the divergent appearance of AA and FA leaves. Aerosols appeared amorphous, as on pine and fir needles, or hazy as on younger oak leaves. The hazy, transparent appearance (figures 4(*c*) and (*e*)) reflected areas of moderate deposition of aerosols, while heavier deposition turned oak leaf surfaces to amorphous, opaque crusts (figure 4(*g*)).

Salts, which are the most hygroscopic component of aerosols, usually deliquesce below 80% RH, doubling their volume with absorbed water (Pilinis *et al* 1989). This process solubilizes and mobilizes salt ions, creates concentration gradients across the leaf surface, and enables the dissolution of trace gases. Assuming homogeneous needle coverage with 5 μg cm^{-2} ionic aerosol (table 3), the absorbed water mass at deliquescence yields a hypothetically homogeneous water film thickness of about 50 nm. Minute amounts of liquid water are sufficient for the dissolution of highly soluble trace gases such as HNO_3 and HCl. Enhanced dissolution in the AA surface solution of HNO_3 likely increased the FA/AA nitrate ratio and acted as an additional nitrate source on fir needles, while a limiting concentration of hygroscopic aerosols in the FA greenhouse may have resulted in higher atmospheric concentrations of HNO_3 and HCl.

SO_2 is only moderately soluble in water. Efficient aqueous oxidation in the atmosphere of SO_2 is generally by H_2O_2 and O_3 (Martin 1984, Seidl 1989). However, in leaf surface water the oxidation of SO_2 by O_2 can be significant, effectively catalyzed by Mn^{2+} ions present in leaf surface water due to substantial leaching from leaves (Burkhardt and Drechsel 1997,

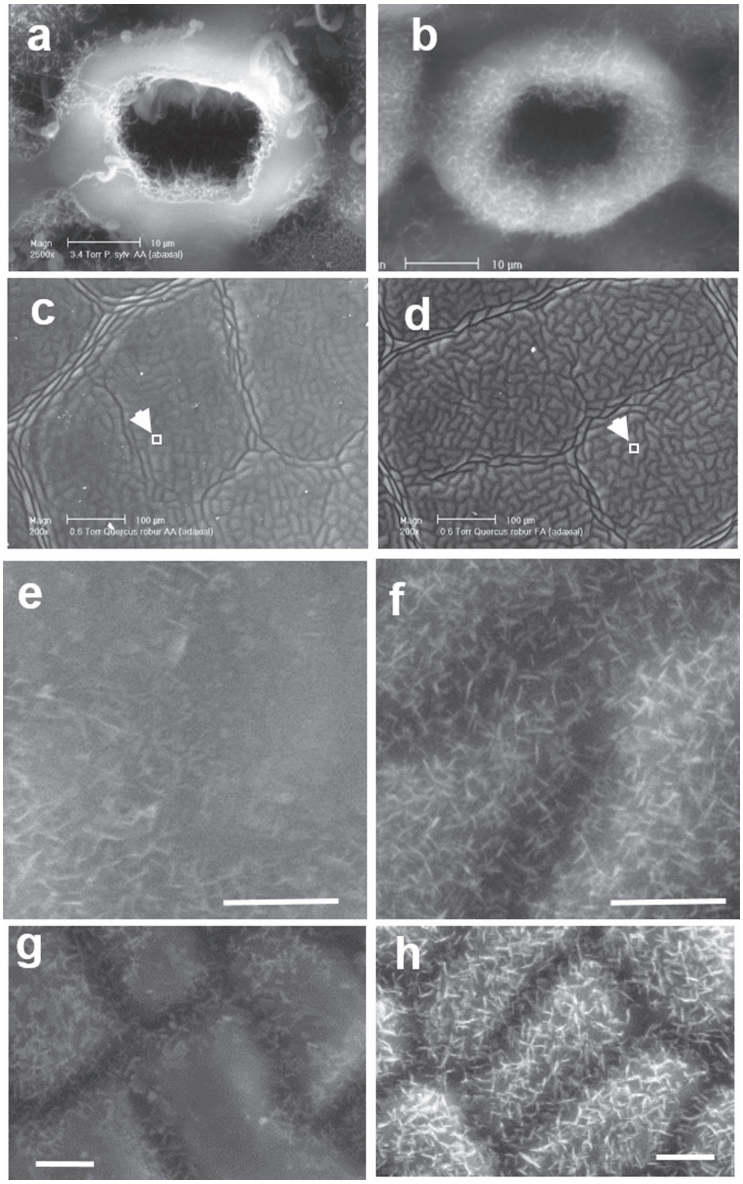

Figure 4. (*a*) and (*b*): Scanning electron microscope (SEM) images of surfaces of Scots pine needles. (*a*): AA, (*b*): FA. (*c*)–(*h*): Common oak leaves. (*c*) and (*e*): AA. (*e*): Detail of (*c*), indicated by white rectangle. (*d*) and (*f*): FA. (*f*): Detail of (*d*), indicated by white rectangle. (*g*): AA, additionally sprayed with Na-fluorescein aerosols of 0.5 μm diameter; (*h*): FA. Scales: (*a*), (*b*), (*e*)–(*h*): 10 μm; (*c*) and (*d*): 100 μm.

Martin 1984, Brandt and van Eldik 1995). Manganese is among the cations most enhanced in throughfall of forest canopies, relative to precipitation (Kreutzer *et al* 1998, Seufert 1990). The sulfuric acid formed on the leaf surface by SO_2 oxidation in turn increases cation leaching; leading to a positive feedback. This may contribute to the previously reported strong correlations of needle Mn content with forest decline symptoms and needle wax quality (Burkhardt and Drechsel 1997, Gärtner *et al* 1990, Seufert 1990, Trimbacher *et al* 1995). Potassium also increased with needle age, and is also strongly leached from leaves (Tukey 1970), contributing to the nearly equal differences between needle age classes observed in AA and FA trees in the present study. Differently from Mn, K was neither depleted nor enhanced below a forest canopy in the eastern US (Lovett and Lindberg 1992), suggesting that leaching and deposition were approximately balanced.

The second, concurrent, aerosol effect was enhanced g_{min}. The g_{min} parameter describes the residual water loss of leaves when stomata are fully closed. It represents the water loss the plant cannot effectively control, and is thus linked to drought tolerance. Increased g_{min} suggests a desiccating impact of ambient aerosols on all three species, which is in line with the recently reported ambient aerosol effects on faba beans (Grantz *et al* 2018). With stomata closed during determination of g_{min}, residual transpiration happens largely by trans-cuticular (TC) or trans-stomatal (TS) liquid water movement. TC liquid water connections are tortuous, and their hydraulic conductance strongly declines with increasing VPD (Fernandez *et al* 2017,

van Gardingen and Grace 1992). In contrast, the existence of TS liquid water connections has been demonstrated by stomatal uptake of nanoparticles (Eichert *et al* 2008). Compared to pure water (Schönherr and Bukovac 1972), deposited aerosols reduce hydrophobicity, and concentrated solutions from deliquescent aerosols can reduce water surface tension (Burkhardt *et al* 2012). Videos obtained by ESEM show that stomatal geometry does not prevent chaotropic ions that disorder water from spreading into stomatal pores (Burkhardt and Hunsche 2013). When these films join with apoplastic water, the hydraulic system of the plant is extended to the leaf surface (HAS, figure 1). Under complete stomatal closure, thin salt crusts with absorbed water vapor may persist and remain active as thin wicks, carrying liquid water between nearly closed guard cells to sites of evaporation at the surface. Increased g_{min} with increasing age or air pollution has often been observed and attributed to leaky (defective or incompletely closed) stomata (Anfodillo *et al* 2002, Burghardt and Riederer 2003, Cape and Fowler 1981, Cape and Percy 1996, Kerstiens 1996, Jordan and Brodribb 2007, Mengel *et al* 1989, Reich 1984, Sase *et al* 1998). This leakiness has been considered as residual transport of water vapor rather than liquid water. While peristomatal TC transport may contribute to g_{min}, an important role for TS flux associated with HAS has fewer chemical and structural constraints. However, while the present results (table 4) together with other studies (Burkhardt and Pariyar 2014, Chappelka and Neufeld 2018, Grantz *et al* 2018, Maier-Maercker and Koch 1992) show a direct impact of particulate air pollutants on plant drought tolerance, the exact pathway of additional water loss remains unclear.

Conditions varied modestly between the two greenhouses. Temperature and VPD were slightly higher in the FA compared to the AA greenhouse, while RH was marginally lower. Lower RH may lead to reduced deliquescence of deposited aerosol in the FA greenhouse. This was minor and dominated by the reduced aerosol deposition in the filtered treatment. Humidity at the leaf surface contributed by stomatal transpiration was also substantial in both treatments. Measurements of g_{min} were made on detached leaves and needles held in darkness in the laboratory, unaffected by VPD differences between the greenhouses. Gaseous concentrations of HNO_3 and HCl were higher in the FA greenhouse, and therefore did not contribute to the greater 'wax degradation' on AA needles.

The microroughness of waxes on the lower surface of silver fir needles collects large amounts of fine aerosols (Burkhardt *et al* 1995). Under natural conditions these are not efficiently removed by rain (Freer-Smith *et al* 2005). This might be an important reason why FDAP started as 'fir decline' in the mid-1970s (Elling *et al* 2007, Schütt 1977, Ulrich 1990). The species lost its well-established drought tolerance and exhibited needle loss, reduced growth, and reduced or completely absent tree rings (Elling *et al* 2009). These symptoms were highly correlated with needle sulfate content, with the symptoms reducing when the air became cleaner by regulatory action (Elling *et al* 2009, Hauck *et al* 2012). Fir suffered more than other species by relatively low concentrations from distant sources, but was relatively tolerant to acute, high SO_2 concentrations (Brenninger and Tranquillini 1983, Elling *et al* 2007). This suggests a reduced role for SO_2 toxicity and a greater role in this species for sulfate aerosols. The formation of particulate material on the leaf surface from gaseous precursors may be an important contributor to the effects documented in the present study.

In the Pyrenees mountains, near the xeric edge of its distribution area, silver fir is currently affected by TMHD (Linares and Camarero 2012, Peguero-Pina *et al* 2011). The species is isohydric, i.e. relying on sensitive stomatal closure in relation to drought. Carbon isotope measurements indicate that fir trees on declining sites had lower intercellular CO_2 concentrations (C_i) and higher intrinsic water use efficiency (WUE_i) than trees on non-declining sites (Linares and Camarero 2012). For plants grown under similar environmental conditions, foliar $\delta^{13}C$ content can be interpreted as a time integrated measure of C_i and WUE_i (Farqhuar and Richards 1984). In the present study, $\delta^{13}C$ values of second year fir needles in the AA greenhouse were less negative than in the FA treatment, indicating reduced C_i and higher WUE_i (see Farquhar and Richards 1984). In contrast, greater g_{min} values indicated increased water loss in AA than FA needles. These conflicting results suggest that HAS (figure 1) may lead to liquid phase transpiration that uncouples $\delta^{13}C$ values from actual WUEi. The isohydric strategy, relying on sensitive stomatal response to VPD and total water loss may thus become less effective under high aerosol loading.

Conclusions

The following conclusions result from this study in the context of other publications:

Hygroscopic action is a primary factor for aerosol impact on plants. The hygroscopic aerosol fraction is mobilized by deliquescence. Creeping salt solutions may expand into the stomata, causing reduced stomatal control and desiccation. This can be recognized in the present study by SEM images (figure 3(*g*), figure 4(*a*)) and by the demonstrated effect on g_{min} (table 4). It is anticipated that the importance of this process increases with (i) increasing aerosol hygroscopicity, which fosters deliquescence and mobility, (ii) increasing chaotropicity, which reduces surface tension, and (iii) the number of deposited aerosols.

Hygroscopic action produces 'wax degradation'. Notwithstanding its well established role as an indicator of forest decline by air pollution (FDAP), the explanatory power of 'wax degradation' as a mechanism

of FDAP has remained low. The multitude of chemical compounds that have been found to produce the symptom (Turunen and Huttunen 1990) suggests that simple chemical reactions are not responsible. The present study shows that aerosol accumulation produces the same SEM images as hypothetical 'wax erosion' or 'wax degradation'. Aerosol accumulation on leaves may be the actual proxy for FDAP.

Hygroscopic action enhances VPD effects on plants. The present study shows that there are consequences of ambient aerosol loading on plant water relations, demonstrated here on g_{min} and previously on g_{min} and flux per unit of stomatal opening (Grantz *et al* 2018). Hygroscopic deposited aerosols react to leaf surface RH. Hydraulically activated stomata (figure 1) cause trans-stomatal liquid water flow and may decrease leaf water potential. Leaf water deficit reduces stomatal aperture, which may reduce CO_2 uptake, but is ineffective in reducing liquid water loss. In isohydric plant species, relying on stomatal closure for protection from atmospheric drought, increased VPD may enhance liquid and vapor phase transpiration, further reducing stomatal conductance and CO_2 uptake. These species may be most vulnerable to tree mortality by hotter drought (TMHD).

Generality of aerosol impacts on plants. In the present and previous studies we have observed similar effects of aerosol deposition, whether ambient or experimentally applied, on a broad range of plant taxa. The measured concentrations of total aerosol and of major ions in the ambient (AA) greenhouse used in this and previous studies were below those observed in many developed and developing countries. The observation of substantial biological effects under these moderate levels of aerosol pollution suggests that potentially stronger effects and greater biological risk may be observed in areas of high concentrations and deposition rates of hygroscopic aerosol.

Acknowledgments

This work was supported by a research grant (BU 1099/7-2) of Deutsche Forschungsgemeinschaft and the project 'Effects of Climate Change on Air Pollution Impacts and Response Strategies for European Ecosystems" ÉCLAIRE, funded under the EC 7th Framework Programme (Grant Agreement No. 282910). We thank I Igrec and J S Sovic for chemical analysis and K Wichterich for his help with scanning electron microscopy. We are grateful to G Welp and A Kiener for assistance with Mn measurements.

ORCID iDs

Juergen Burkhardt https://orcid.org/0000-0001-6539-1143

References

Adams H D *et al* 2017 A multi-species synthesis of physiological mechanisms in drought-induced tree mortality *Nat. Ecol. Evol.* **1** 1285–91

Allen C D, Breshears D D and McDowell N G 2015 On underestimation of global vulnerability to tree mortality and forest die-off from hotter drought in the Anthropocene *Ecosphere* **6** 129

Andreae M O 2007 Aerosols before pollution *Science* **315** 50–1

Anfodillo T, Di Bisceglie D P and Urso T 2002 Minimum cuticular conductance and cuticle features of *Picea abies* and *Pinus cembra* needles along an altitudinal gradient in the Dolomites (NE Italian Alps) *Tree Physiol.* **22** 479–87

Bigler C, Braker O U, Bugmann H, Dobbertin M and Rigling A 2006 Drought as an inciting mortality factor in Scots pine stands of the Valais, Switzerland *Ecosystems* **9** 330–43

Brandt C and Van Eldik R 1995 Transition-metal-catalyzed oxidation of sulfur(IV) oxides - atmospheric-relevant processes and mechanisms *Chem. Rev.* **95** 119–90

Brenninger C and Tranquillini W 1983 Photosynthesis, transpiration and stomatal response of various species of woody-plants exposed to sulfur-dioxide *Eur. J. Forest Pathol.* **13** 228–38

Breshears D D *et al* 2005 Regional vegetation die-off in response to global-change-type drought *Proc. Natl Acad. Sci. USA* **102** 15144–8

Buras A *et al* 2018 Are Scots pine forest edges particularly prone to drought-induced mortality? *Environ. Res. Lett.* **13** 025001

Burghardt M and Riederer M 2003 Ecophysiological relevance of cuticular transpiration of deciduous and evergreen plants in relation to stomatal closure and leaf water potential *J. Exp. Bot.* **54** 1941–9

Burkhardt J 2010 Hygroscopic particles on leaves: nutrients or desiccants? *Ecol. Monogr.* **80** 369–99

Burkhardt J, Basi S, Pariyar S and Hunsche M 2012 Stomatal penetration by aqueous solutions—an update involving leaf surface particles *New Phytol.* **196** 774–87

Burkhardt J and Drechsel P 1997 The synergism between SO_2 oxidation and manganese leaching on spruce needles - a chamber experiment *Environ. Pollut.* **95** 1–11

Burkhardt J and Eiden R 1994 Thin water films on coniferous needles *Atmos. Environ.* **28** 2001–11

Burkhardt J and Grantz D A 2017 Plants and atmospheric aerosols *Progress in Botany* ed F M Cánovas and R Matyssek vol 8 (Cham: Springer) pp 369–406

Burkhardt J and Hunsche M 2013 'Breath figures' on leaf surfaces—formation and effects of microscopic leaf wetness *Front. Plant Sci.* **4** 422

Burkhardt J, Kaiser H, Goldbach H and Kappen L 1999 Measurements of electrical leaf surface conductance reveal recondensation of transpired water vapour on leaf surfaces *Plant Cell Environ.* **22** 189–96

Burkhardt J, Kaiser H, Kappen L and Goldbach H E 2001 The possible role of aerosols on stomatal conductivity for water vapour *Basic Appl. Ecol.* **2** 351–64

Burkhardt J and Pariyar S 2014 Particulate pollutants are capable to 'degrade' epicuticular waxes and to decrease the drought tolerance of Scots pine (*Pinus sylvestris* L.) *Environ. Pollut.* **184** 659–67

Burkhardt J and Pariyar S 2016 How does the VPD response of isohydric and anisohydric plants depend on leaf surface particles? *Plant Biol.* **18** 91–100

Burkhardt J, Peters K and Crossley A 1995 The presence of structural surface waxes on coniferous needles affects the pattern of dry deposition of fine particles *J. Exp. Bot.* **46** 823–31

Bussotti F and Ferretti M 1998 Air pollution, forest condition and forest decline in southern Europe: an overview *Environ. Pollut.* **101** 49–65

Cape J N and Fowler D 1981 Changes in epicuticular wax of *Pinus sylvestris* exposed to polluted air *Silva Fennica* **15** 457–8

Cape J N and Percy K E 1996 The interpretation of leaf-drying curves *Plant Cell Environ.* **19** 356–61
Chappelka A H and Neufeld H S 2018 A link between physical and chemical climate change: the enhancement of vegetative water loss by atmospheric aerosols *New Phytol.* **219** 9–11
Eichert T, Kurtz A, Steiner U and Goldbach H E 2008 Size exclusion limits and lateral heterogeneity of the stomatal foliar uptake pathway for aqueous solutes and water-suspended nanoparticles *Physiol. Plant.* **134** 151–60
Elling W, Dittmar C, Pfaffelmoser K and Rotzer T 2009 Dendroecological assessment of the complex causes of decline and recovery of the growth of silver fir (*Abies alba* Mill.) in southern Germany *Forest Ecol. Manage.* **257** 1175–87
Elling W, Heber U, Polle A and Beese F 2007 *Schädigung von Waldökosystemen* (München: Elsevier) p 422
Farquhar G D and Richards R A 1984 Isotopic composition of plant carbon correlates with water-use efficiency of wheat genotypes *Aust. J. Plant Physiol.* **11** 539–52
Fernandez V, Bahamonde H A, Peguero-Pina J J, Gil-Pelegrin E, Sancho-Knapik D, Gil L, Goldbach H E and Eichert T 2017 Physico-chemical properties of plant cuticles and their functional and ecological significance *J. Exp. Bot.* **68** 5293–306
Freer-Smith P H, Beckett K P and Taylor G 2005 Deposition velocities to *Sorbus aria, Acer campestre, Populus deltoides X trichocarpa Beaupre, Pinus nigra* and *X Cupressocyparis leylandii* for coarse, fine and ultra-fine particles in the urban environment *Environ. Pollut.* **133** 157–67
Gärtner E J, Urfer W, Eichhorn J, Grabowski H and Huss H 1990 Mangan - ein Bioindikator für den derzeitigen SChadzustand mittelalter Fichten in Hessen *Forstarchiv* **61** 229–33
Grantz D A, Zinsmeister D and Burkhardt J 2018 Ambient aerosol increases minimum leaf conductance and alters the aperture-flux relationship as stomata respond to VPD *New Phytol.* **219** 279–86
Hauck M, Zimmermann J, Jacob M, Dulamsuren C, Bade C, Ahrends B and Leuschner C 2012 Rapid recovery of stem increment in Norway spruce at reduced SO_2 levels in the Harz Mountains, Germany *Environ. Pollut.* **164** 132–41
Huang B J and Huang J C 1976 Creeping-film phenomenon of potassium-chloride solution *Nature* **261** 36–8
Jordan G J and Brodribb T J 2007 Incontinence in aging leaves: deteriorating water relations with leaf age in Agastachys odorata (Proteaceae), a shrub with very long-lived leaves *Funct. Plant Biol.* **34** 918–24
Johnson A H and Siccama T G 1983 Acid deposition and forest decline *Environ. Sci. Technol.* **17** A294–A305
Kerstiens G 1996 Cuticular water permeability and its physiological significance *J. Exp. Bot.* **47** 1813–32
Klap J M, Voshaar J H O, De Vries W and Erisman J W 2000 Effects of environmental stress on forest crown condition in Europe. Part IV: statistical analysis of relationships *Water Air Soil Pollut.* **119** 387–420
Kreutzer K *et al* 1998 Atmospheric deposition and soil acidification in five coniferous forest ecosystems: a comparison of the control plots of the EXMAN sites *Forest Ecol. Manage.* **101** 125–42
Linares J C and Camarero J J 2012 From pattern to process: linking intrinsic water-use efficiency to drought-induced forest decline *Glob. Change Biol.* **18** 1000–15
Lovett G M and Lindberg S E 1992 Concentration and deposition of particles and vapors in a vertical profile through a forest canopy *Atmos. Environ. Part A* **26** 1469–76
Ludwig J and Klemm O 1990 Acidity of size-fractionated aerosol-particles *Water Air Soil Pollut.* **49** 35–50
Maier-Maercker U and Koch W 1992 The effect of air-pollution on the mechanism of stomatal control *Trees-Struct. Funct.* **7** 12–25
Martin L R 1984 Kinetic studies of sulfite oxidation in aqueous solution *SO_2, NO and NO_2 Oxidation Mechanisms: Atmospheric Considerations* ed J G Matyssek (Boston: Butterworth) pp 63–100
McDowell N *et al* 2008 Mechanisms of plant survival and mortality during drought: why do some plants survive while others succumb to drought? *New Phytol.* **178** 719–39
McLaughlin S B 1985 Effects of air-pollution on forests—a critical review *J. Air Pollut. Contr. Assoc.* **35** 512–34
Mengel K, Hogrebe A M R and Esch A 1989 Effect of acidic fog on needle surface and water relations of *Picea abies Physiol. Plant.* **75** 201–7
Novick K A *et al* 2016 The increasing importance of atmospheric demand for ecosystem water and carbon fluxes *Nat. Clim. Change* **6** 1023–7
Pariyar S, Eichert T, Goldbach H E, Hunsche M and Burkhardt J 2013 The exclusion of ambient aerosols changes the water relations of sunflower (*Helianthus annuus*) and bean (*Vicia faba*) plants *Environ. Exp. Bot.* **88** 43–52
Patrut A, Woodborne S, Patrut R T, Rakosy L, Lowy D A, Hall G and von Reden K F 2018 The demise of the largest and oldest African baobabs *Nat. Plants* **7** 423–6
Peguero-Pina J J, Sancho-Knapik D, Cochard H, Barredo G, Villarroya D and Gil-Pelegrin E 2011 Hydraulic traits are associated with the distribution range of two closely related mediterranean firs, *Abies alba* Mill. and *Abies pinsapo* Boiss *Tree Physiol.* **31** 1067–75
Petters M D and Kreidenweis S M 2007 A single parameter representation of hygroscopic growth and cloud condensation nucleus activity *Atmos. Chem. Phys.* **7** 1961–71
Pilinis C, Seinfeld J H and Grosjean D 1989 Water content of atmospheric aerosols *Atmos. Environ.* **23** 1601–6
Putaud J P *et al* 2010 A European aerosol phenomenology-3: physical and chemical characteristics of particulate matter from 60 rural, urban, and kerbside sites across Europe *Atmos. Environ.* **44** 1308–20
Reich P B 1984 Loss of stomatal function in aging hybrid poplar leaves *Ann. Bot.* **53** 691–8
Sase H, Takamatsu T, Yoshida T and Inubushi K 1998 Changes in properties of epicuticular wax and the related water loss in Japanese cedar (*Cryptomeria japonica*) affected by anthropogenic environmental factors *Can. J. Forest Res.* **28** 546–56
Schönherr J and Bukovac M J 1972 Penetration of stomata by liquids - dependence on surface tension, wettability, and stomatal morphology *Plant Physiol.* **49** 813–9
Schulze E D 1989 Air-pollution and forest decline in a Spruce (*Picea-Abies*) forest *Science* **244** 776–83
Schütt P 1977 Silver-fir decline *Forstwiss. Centralbl.* **96** 177–86
Schütt P and Cowling E B 1985 Waldsterben, a general decline of forests in Central Europe—symptoms, development and possible causes *Plant Dis.* **69** 548–58
Seidl W 1989 Ionic concentrations and initial S(IV)-oxidation rates in droplets during the condensational stage of cloud *Tellus B* **41** 32–50
Seufert G 1990 Flow-rates of ions in waters percolating through a model ecosystem with forest trees *Environ. Pollut.* **68** 231–52
Steffen W *et al* 2015 Planetary boundaries: guiding human development on a changing planet *Science* **347** 736
Tang Y S *et al* 2009 European scale application of atmospheric reactive nitrogen measurements in a low-cost approach to infer dry deposition fluxes *Agric. Ecosys. Environ.* **133** 183–95
Trimbacher C, Eckmüllner O and Weiss P 1995 *Die Wachsqualität von Fichtennadeln österreichischer Hintergrundstandorte Umweltbundesamt* vol 057 (Umweltbundesamt GmbH: Wien, Austria, Monographien)) p 119
Trimbacher C and Weiss P 1999 Needle surface characteristics and element contents of Norway spruce in relation to the distance of emission sources *Environ. Pollut.* **105** 111–9
Tukey H B 1970 Leaching of substances from plants *Annu. Rev. Plant Physiol.* **21** 305–24
Turunen M and Huttunen S 1990 A review of the response of epicuticular wax of conifer needles to air pollution *J. Environ. Qual.* **19** 35–45

Ulrich B 1990 Waldsterben - forest decline in West-Germany *Environ. Sci. Technol.* **24** 436–41

Vacek S, Hunova I, Vacek Z, Hejcmanova P, Podrazsky V, Kral J, Putalova T and Moser W K 2015 Effects of air pollution and climatic factors on Norway spruce forests in the Orlick, Hory Mts. (Czech Republic), 1979–2014 *Eur. J. Forest Res.* **134** 1127–42

van Enckevort W J P and Los J H 2013 On the creeping of saturated salt solutions *Cryst. Growth Des.* **13** 1838–48

van Gardingen P R and Grace J 1992 Vapor-pressure deficit response of cuticular conductance in intact leaves of *fagus-sylvatica L. J. Exp. Bot.* **43** 1293–9

van Mantgem P J *et al* 2009 Widespread increase of tree mortality rates in the Western United States *Science* **323** 521–4

Williams A P *et al* 2013 Temperature as a potent driver of regional forest drought stress and tree mortality *Nat. Clim. Change* **3** 292–7